
Provably Bounding Neural Network Preimages

Suhas Kotha

Carnegie Mellon

suhask@andrew.cmu.edu

Christopher Brix

RWTH Aachen

Zico Kolter

Carnegie Mellon

Bosch Center for AI

Krishnamurthy (Dj) Dvijotham*

Google Research, Brain Team

Huan Zhang*

Carnegie Mellon

Abstract

Most work on the formal verification of neural networks has focused on bounding forward images of neural networks, i.e., the set of outputs of a neural network that correspond to a given set of inputs (for example, bounded perturbations of a nominal input). However, many use cases of neural network verification require solving the inverse problem, i.e., over-approximating the set of inputs that lead to certain outputs. In this work, we present the first efficient bound propagation algorithm, INVPROP, for verifying properties over the preimage of a linearly constrained output set of a neural network, which can be combined with branch-and-bound to achieve completeness. Our efficient algorithm allows multiple passes of intermediate bound refinements, which are crucial for tight inverse verification because the bounds of an intermediate layer depend on relaxations both before and after this layer. We demonstrate our algorithm on applications related to quantifying safe control regions for a dynamical system and detecting out-of-distribution inputs to a neural network. Our results show that in certain settings, we can find over-approximations that are over $2500\times$ tighter than prior work while being $2.5\times$ faster on the same hardware.

1 Introduction

Applications of neural networks to safety-critical settings often require reasoning about the set of inputs that will produce a particular set of outputs. For example, for a physical system controlled by a policy parameterized as a neural network, it is of interest to understand the states that would cause the policy to choose control actions that are outside acceptable limits (for example torques that are beyond the safe operating range of a motor), or that would result in a future state that violates safety constraints. Another example is quantifying the out-of-distribution (OOD) detection behavior of a neural network: here, it is of interest to bound the set of inputs that leads to a classifier making a confident prediction, i.e., where the highest scoring logit exceeds the second highest scoring logit by a large margin. Given this set, one can assess whether there are inputs far from the training data that are assigned high confidence predictions, which would be an undesirable property.

Formal verification of neural networks seeks to provide provable guarantees demonstrating that networks satisfy formal specifications on their inputs and outputs. Practical algorithms often rephrase the above as finding provably correct bounds on the inputs or outputs of a neural network subject to specific constraints. Most work to date has focused on developing algorithms that can bound the outputs of a neural network given constraints on the inputs, which is challenging due to high

*Equal contribution

Code is available at <https://github.com/kothasuhas/verify-input>

dimensionality and non-convexity. For example, to analyze the robustness of a neural network to perturbations of a given input, these algorithms compute bounds on the outputs of the network given that the inputs are bounded perturbations of a nominal input [Wong and Kolter, 2018, Dvijotham et al., 2018, Zhang et al., 2018, Raghunathan et al., 2018, Gehr et al., 2018].

In this work, we address the inverse problem, motivated by the use-cases outlined above. Our goal is to find bounds on the pre-image of a neural network: given a set of outputs \mathcal{S}_{out} (described by linear constraints on the output of a neural network), we seek to find a set that provably contains all inputs that lead to such outputs. The verification problem is already challenging due to non-convexity and high dimensionality. This new problem is increasingly difficult since neural networks are not invertible.

Specifically, representative efficient verifiers (such as state of the art bound-propagation-based methods [Zhang et al., 2022]) can only compute bounds in the forward direction, and the tightness of the linear programming relaxations they rely on to perform formal verification critically depends on having tight bounds on intermediate activations. In the setting of this paper, however, the bounds available on the intermediate activations derived from the input constraints are weak, since the only constraints on the input are that it should be from the valid input domain (for example, normalized pixels from an image lie between 0 and 1). In fact, in some applications like control, the input domain may be unbounded. Given this, the bounds on intermediate activations derived from the input constraints may be vacuous or very loose, impacting the tightness of the intermediate activation relaxations. We efficiently solve this problem by significantly generalizing the existing bound propagation-based verification framework. Our contributions are as follows:

- We formulate the *inverse verification problem* for neural networks, i.e, the problem of over-approximating the set of inputs that leads to a given set of outputs, with a mixed integer linear programming formulation. This motivates our development of an efficient bound propagation method.
- We develop an effective bound propagation framework, Inverse Propagation for Neural Network Verification (INVPROP), which computes provable over-approximations of neural network preimages. We study the convex outer approximation of this problem which leads to a novel inverse bound propagation method for verification. We also unify INVPROP and forward verification bound propagation into a more general verification framework, allowing us to connect our method to standard tools and benefit from prior progress in the verification community, such as efficient GPU acceleration.
- We demonstrate that tight inverse verification requires multiple refinement passes of intermediate bounds. This is unique to the inverse verification problem because bounds for an intermediate layer depend on not only intermediate bounds before this layer, but also constraints imposed on downstream layers or the output of the network. In other words, bounds cannot be simply propagated in a single forward pass first tightening all neurons in a given layer and then tightening the next layer based on the previous layer bounds. Instead, inverse verification requires an iterative process where, in each pass, all bounds are tightened based on previous bounds (including output constraints), and the iterative process continues until bounds converge.
- We improve the state-of-the-art on a control benchmark Rober et al. [2022a,b] by providing $2500 \times$ tighter bounds with $2.5 \times$ faster computation. We also demonstrate applicability in OOD detection.

2 Setup

2.1 Notation

Throughout this paper, we will use $[L]$ for $L \in \mathbb{N}$ to refer to the set $\{1, 2, \dots, L\}$, $\mathbf{W}_{:,j}^{(i)}$ to refer to column j of the matrix $\mathbf{W}^{(i)}$, $[\cdot]_+$ to refer to $\max(0, \cdot)$, and $[\cdot]_-$ to refer to $-\min(0, \cdot)$. We will also boldface symbols for vectors and matrices (such as $\mathbf{x}^{(i)}$ and $\mathbf{W}^{(i)}$) and use regular symbols for scalars (such as $x_j^{(i)}$). We use $\mathbf{x} \odot \mathbf{y}$ to denote element-wise multiplication of vectors \mathbf{x}, \mathbf{y} .

We define an L layer ReLU neural network by its weight matrices $\mathbf{W}^{(i)}$ and bias vectors $\mathbf{b}^{(i)}$ for $i \in [L]$. The output of the neural network for the input $\hat{\mathbf{x}}^{(0)}$ from a bounded input domain \mathcal{X} is computed by alternately applying linear layers $\mathbf{x}^{(i)} = \mathbf{W}^{(i)}\hat{\mathbf{x}}^{(i-1)} + \mathbf{b}^{(i)}$ and ReLU layers

$\hat{\mathbf{x}}^{(i)} = \max(\mathbf{0}, \mathbf{x}^{(i)})$ until we receive the output $\mathbf{x}^{(L)}$ (which we refer to as the logits). Note that we treat softmax as a component of the loss function, not the neural network.

The inputs to our network will lie in the Euclidean space \mathbb{R}^{in} and the outputs will lie in \mathbb{R}^{out} . For any subset S of \mathbb{R}^d (d dimensional Euclidean space), $\text{CONV}(S)$ denotes the convex hull of S , i.e, the smallest convex set containing S .

2.2 Problem Statement

Given a neural network $f : \mathcal{X} \subseteq \mathbb{R}^{\text{in}} \rightarrow \mathbb{R}^{\text{out}}$ and an output constraint $\mathcal{S}_{\text{out}} \subseteq \mathbb{R}^{\text{out}}$, we want to compute $f^{-1}(\mathcal{S}_{\text{out}}) \subseteq \mathcal{X}$. Precisely computing or expressing $f^{-1}(\mathcal{S}_{\text{out}})$ is an intractable problem in general. Therefore, we strive to compute a tight over-approximation $\mathcal{S}_{\text{over}}$ such that $f^{-1}(\mathcal{S}_{\text{out}}) \subseteq \mathcal{S}_{\text{over}}$. In particular, we will develop an algorithm to compute $\mathcal{S}_{\text{over}} = \text{CONV}(f^{-1}(\mathcal{S}_{\text{out}}))$, the convex hull of the pre-image, via a cutting-plane representation. In this paper, \mathcal{S}_{out} will always be defined by a set of linear constraints parameterized by $\mathbf{H}f(\mathbf{x}) + \mathbf{d} \leq \mathbf{0}$.

2.3 Applications

We outline two concrete applications of our approach.

Backward Reachability Analysis for Neural Feedback Loops. For control problems involving linear dynamical systems with quadratic cost functions, the optimal feedback policies can be proven to be linear Bertsekas [2000]. However, many tasks require non-quadratic cost functions (for example, tasks requiring driving a system towards a desired safe set). In this case, linear feedback policies are no longer sufficient. Neural networks constitute a flexible class of nonlinear feedback policies. However, establishing safety guarantees for neural network policies is a challenging task. In particular, one problem of interest is to find a set of initial states that does not reach a particular set of future states under the neural network policy. This can be helpful in collision avoidance or control with safety constraints.

Under linear time-invariant dynamics, the state of a system is determined by the state transition function

$$\mathbf{x}_{t+1} = f(\mathbf{x}_t) = \mathbf{A}\mathbf{x}_t + \mathbf{B}\pi(\mathbf{x}_t) + \mathbf{c}$$

where for $x_n, x_u \in \mathbb{N}$, $\mathbf{x}_t \in \mathcal{X} \subseteq \mathbb{R}^{x_n}$ is the state at discrete timestep t , $\mathbf{A} \in \mathbb{R}^{x_n \times x_n}$ and $\mathbf{B} \in \mathbb{R}^{x_n \times n_u}$ are known system matrices, $\mathbf{c} \in \mathbb{R}^{x_n}$ is a known exogenous input, and $\pi : \mathcal{X} \rightarrow \mathbb{R}^{n_u}$ is the state-feedback control policy (the decision the model takes given the state).

In the controls benchmark we use for our evaluation Hu et al. [2020], Everett et al. [2021, 2022], a robot is moving on the floor of a room with coordinates spanning $\mathcal{X} = [-5, 5] \times [-5, 5]$. The position of the robot at time $t + 1$ can be directly computed based on the position at time t , and follows the equation

$$\mathbf{x}_{t+1} = f(\mathbf{x}_t) = \begin{bmatrix} 1 & 1 \\ 0 & 1 \end{bmatrix} \mathbf{x}_t + \begin{bmatrix} 0.5 \\ 1 \end{bmatrix} \pi(\mathbf{x}_t)$$

with $\pi : \mathbb{R}^2 \rightarrow \mathbb{R}$. There is an obstacle in the room covering the region $[4.5, 5.0] \times [-0.25, 0.25]$ that the robot needs to avoid. It is of interest to understand whether, starting in a given state, the system will enter the unsafe region in the next time-step. We can represent this obstacle set with the linear constraints

$$\mathcal{S}_{\text{out}} = \left\{ \mathbf{x}_{t+1} : \begin{bmatrix} -1 & 0 \\ 0 & -1 \\ 1 & 0 \\ 0 & 1 \end{bmatrix} \mathbf{x}_{t+1} + \begin{bmatrix} 4.5 \\ -0.25 \\ -5.0 \\ -0.25 \end{bmatrix} \leq \begin{bmatrix} 0 \\ 0 \\ 0 \\ 0 \end{bmatrix} \right\}$$

$f^{-1}(\mathcal{S}_{\text{out}})$ denotes the set of states \mathbf{x}_t such that \mathbf{x}_{t+1} lies in the unsafe region given the control policy π . Overapproximating this set allows us to define the set of states to avoid one timestep in advance. We can compose f with itself t times to obtain the set of initial states where π would drive the system to the unsafe set after t steps.

Computing the set of inputs that leads to confident predictions. Training a classifier that knows when it doesn’t know is a challenging problem. A simple and effective approach to doing this is to train a classifier with an additional logit representing (out of distribution) OOD-ness. Labeled data for this additional class is generated via outlier exposure, i.e., adding synthetic training data with features drawn from an OOD distribution (known as outlier exposure [Hendrycks et al., 2018]) and labels corresponding to the additional OOD logit [Chen et al., 2021].

Consider the logits y produced by a classifier trained in this manner for a binary classification task. The classifier can classify in-distribution data by comparing y_0 and y_1 , the logits corresponding to the two in-distribution labels. The quantity $\max(y_0, y_1) - y_2$, known as the logit gap, can be used to identify out-of-distribution data (Fig. 1).

A natural question to ask is: Can it correctly identify datapoints far from the training data as being OOD? In order to do so, one needs to compute the preimage of the set

$$\mathcal{S}_{\text{out}} = \{y : \max(y_0, y_1) \geq y_2\}$$

We detail how to model this set with linear constraints in Section D.1. The algorithm INVPROP we develop in this paper enables us to compute an overapproximation of $f^{-1}(\mathcal{S}_{\text{out}})$, thereby answering the question of whether the classifier learned to correctly identify OOD data.

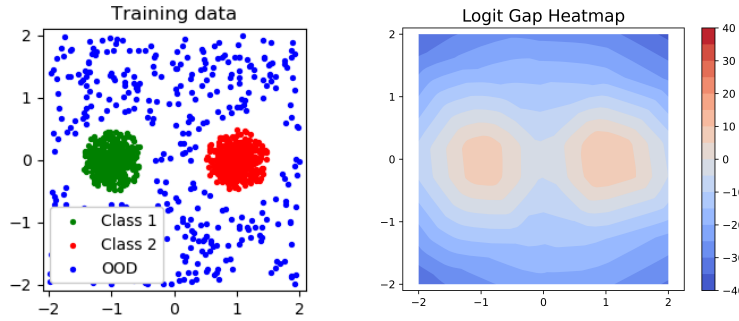


Figure 1: To improve our model’s ability to detect data outside the training distribution (of green and red points), we randomly sample points that are far from every training point. In the right contour, we see that the model’s confidence of in-distribution increases as we approach the centers of the distribution, demonstrating our model is more calibrated.

3 Approach

We first provide an algorithm to find convex over-approximations of feed-forward ReLU networks. We then extend our method to non-convex over-approximations of general computational graphs.

3.1 Convex over-approximation

Suppose we want to find a convex over-approximation of $f^{-1}(\mathcal{S}_{\text{out}})$. The tightest such set is its convex hull, which is the intersection of all half-spaces that contain $f^{-1}(\mathcal{S}_{\text{out}})$ [Boyd et al., 2004]. This intersection is equivalent to $\bigcap_{c \in \mathbb{R}^n} \{x : c^\top x \geq \min_{f(x') \in \mathcal{S}_{\text{out}}} c^\top x'\}$, which means that we can build an over-approximation by taking this intersection for finitely many c . Furthermore, replacing the minimization problem with a lower bound to its value still yields a valid half-space, where a tighter bound yields a tighter approximation.

We focus on convex over-approximations for two reasons: First, checking that the pre-image satisfies a linear constraint $c^\top x + d \geq 0$ is equivalent to minimizing the linear function $x \mapsto c^\top x$ over the pre-image, which is in turn equivalent to minimizing the linear function over $\text{CONV}(f^{-1}(\mathcal{S}_{\text{out}}))$ [Boyd et al., 2004]. Second, the convex hull and its tractable over-approximations are conveniently represented as intersections of linear constraints on the pre-image, each of which can be quickly computed after a single precomputation phase to tighten bounds on intermediate neurons using the INVPROP algorithm outlined in the next section.

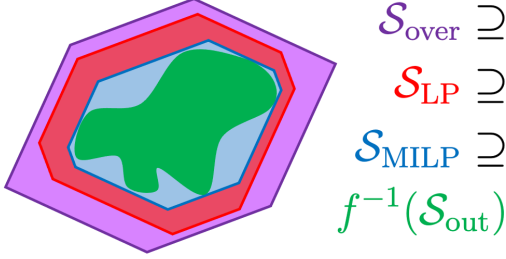


Figure 2: Visualization of relaxations. The inner green region depicts the true $f^{-1}(\mathcal{S}_{\text{out}})$, the blue relaxation depicts the intersection of finite half-spaces solved via MILP, the red relaxation displays the same via LP, and the purple relaxation displays the same via INVPROP.

For the above reasons, we will focus on solving the following constrained optimization problem.

$$\min_{\mathbf{x}} \quad \mathbf{c}^\top \mathbf{x} \quad (1a)$$

$$\text{s.t.} \quad \mathbf{x} \in \mathcal{X}; \quad f(\mathbf{x}) \in \mathcal{S}_{\text{out}} \quad (1b)$$

Note that this differs from the forward verification problem widely studied in the literature, which can be phrased as

$$\min_{\mathbf{x} \in \mathcal{S}_{\text{in}}} \quad \mathbf{c}^\top f(\mathbf{x})$$

where \mathcal{S}_{in} is a set representing constraints on the input, and the goal of the verification is to establish that the output $f(\mathbf{x})$ satisfies a linear constraint of the form $\mathbf{c}^\top f(\mathbf{x}) \geq d$ for all $\mathbf{x} \in \mathcal{S}_{\text{in}}$.

3.2 The INVPROP Algorithm

As a brief overview of our method, we first construct the Mixed Integer Linear Program (MILP) for solving this optimization problem, which generates the over-approximation $\mathcal{S}_{\text{MILP}}$ when solved for finitely many \mathbf{c} . Then, we relax the MILP to a Linear Program (LP), which can construct the over-approximation \mathcal{S}_{LP} . Finally, we relax the LP via its Lagrangian dual, which will be used to construct our over-approximation $\mathcal{S}_{\text{over}}$. This chain of relaxations is visualized in Figure 2. Though the diagram displays looseness, in the coming sections we provide a comprehensive methodology to arbitrarily reduce error in all three relaxations.

The Mixed Integer Linear Programming (MILP) Formulation For feed-forward neural networks with ReLU non-linearities, this problem admits a MILP encoding similar to prior work in adversarial robustness Tjeng et al. [2017]. The weights and biases at layer i are denoted by $\mathbf{W}^{(i)}, \mathbf{b}^{(i)}$. Let $\hat{\mathbf{x}}^{(i)}$ denote the post-activations (following the application of the ReLU nonlinearity) at layer i and $\mathbf{x}^{(i)}$ denote the pre-activations. Then, the problem (1) is equivalent to:

$$\min_{\mathbf{x}, \hat{\mathbf{x}}, \mathbf{z}} \quad \mathbf{c}^\top \mathbf{x} \quad (2a)$$

$$\text{s.t.} \quad \mathbf{x} \in \mathcal{X}; \quad \hat{\mathbf{x}}^{(0)} = \mathbf{x}; \quad \mathbf{H}\mathbf{x}^{(L)} + \mathbf{d} \leq \mathbf{0} \quad (2b)$$

$$\mathbf{x}^{(i)} = \mathbf{W}^{(i)}\hat{\mathbf{x}}^{(i-1)} + \mathbf{b}^{(i)}; \quad i \in [L], \quad (2c)$$

$$\hat{\mathbf{x}}^{(i)} = \max(0, \mathbf{x}^{(i)}); \quad i \in [L-1] \quad (2d)$$

We note that, as opposed to prior work on verifying forward properties of neural networks [Zhang et al., 2022], our approach seeks to bound a linear function of the *inputs* to the neural network, subject to constraints on the *output* of the neural network. This makes it particularly challenging to directly apply bound propagation algorithms derived in prior work, as these algorithms rely on propagating bounds on the inputs to obtain tight bounds on intermediate activations. In our problem, we need to modify these algorithms to leverage constraints on the outputs of downstream layers to obtain bounds on intermediate or input neurons.

Figure 3: A simple neural network from \mathbb{R} to \mathbb{R} . Every node is the sum of its incoming nodes unless the edge is labeled ReLU.

The Linear Programming (LP) Formulation Unfortunately, finding an exact solution to this MILP is NP-complete Katz et al. [2017]. To sidestep the intractability of exact verification, we can compute lower bounds for this program via its convex relaxation. In order to do so, we begin by finding bounds on the outputs of intermediate layers:

$$l_j^{(i)} \leq x_j^{(i)} \leq u_j^{(i)}$$

Based on these bounds, we can rewrite the last constraint of (2) as follows:

$$\begin{aligned} 0 \leq \hat{x}_j^{(i)} &\leq u_j^{(i)} z_j^{(i)} \\ x_j^{(i)} \leq \hat{x}_j^{(i)} &\leq x_j^{(i)} - l_j^{(i)}(1 - z_j^{(i)}) \end{aligned} \quad z_j^{(i)} \in \{0, 1\}$$

Relaxing the constraints on z to $z_j^{(i)} \in [0, 1]$, we obtain the following LP relaxation of (2):

$$\min_{\mathbf{x}, \hat{\mathbf{x}}, \mathbf{z}} \mathbf{c}^\top \mathbf{x} \quad (3a)$$

$$\text{s.t. } \mathbf{x} \in \mathcal{X}; \mathbf{l}^{(0)} \leq \mathbf{x} \leq \mathbf{u}^{(0)}; \hat{\mathbf{x}}^{(0)} = \mathbf{x} \quad (3b)$$

$$\mathbf{Hx}^{(L)} + \mathbf{d} \leq \mathbf{0} \quad (3c)$$

$$\mathbf{x}^{(i)} = \mathbf{W}^{(i)} \hat{\mathbf{x}}^{(i-1)} + \mathbf{b}^{(i)}; \quad i \in [L], \quad (3d)$$

$$\mathbf{0} \leq \hat{\mathbf{x}}^{(i)} \leq \mathbf{u}^{(i)} \odot \mathbf{z}^{(i)} \quad i \in [L] \quad (3e)$$

$$\mathbf{x}^{(i)} \leq \hat{\mathbf{x}}_j^{(i)} \leq \mathbf{x}^{(i)} - \mathbf{l}^{(i)} \odot (1 - \mathbf{z}^{(i)}) \quad i \in [L], \quad (3f)$$

$$\mathbf{0} \leq \mathbf{z}^{(i)} \leq \mathbf{1} \quad i \in [L] \quad (3g)$$

where the bounds $\mathbf{l}^{(0)} \leq \mathbf{x} \leq \mathbf{u}^{(0)}$ are either the bounds already implicit in \mathcal{X} , or a refinement of these obtained via previous rounds of bound propagation or input branching (see Algorithm 1).

Most efficient neural network verifiers do not solve an LP formulation of verification directly because LP solvers are often slow for problem instances involving neural networks. Instead, the bound propagation framework [Zhang et al., 2018, Wang et al., 2021, Zhang et al., 2022] is a practical and efficient way to lower bound the LP relaxation of the forward verification problem. However, there are *two major roadblocks* to applying existing methods here: First, typical methods cannot directly handle the output constraints (Eq. 3c) and the objective involving input layer variables (Eq. 3a); second, the intermediate bounds \mathbf{l} and \mathbf{u} must be computed considering the output constraint (Eq. 3c), which is impossible with existing bound propagation methods, as discussed below.

Example 1. Consider the toy neural network in Figure 3 under $\mathcal{X} = [-2, 2]$ and $\mathcal{S}_{\text{out}} = \{y : 1 \leq y \leq 1.02\}$. Suppose we wanted to find the tightest $[l_0^{(1)}, u_0^{(1)}]$ (bounds on $x_0^{(1)}$). If we only enforce the constraints preceding the ReLU (standard bound propagation), we get $[-2, 2]$. If we only enforce the constraints following the ReLU, we get $(-\infty, 1.02]$. However, when we utilize all of the constraints, we find that the true intermediate bounds are $[0, 0.01]$, which is over 100 times tighter than the intersection of the two previous methods (all derivations provided in Appendix C). Therefore, new techniques are necessary for optimizing intermediate bounds in this setting.

The Inverse Propagation (INVPROP) Formulation By changing the LP in Section 3.2 to optimize the quantity $\hat{x}_j^{(0)}$ or $x_j^{(i)}$ for $i \in [L-1]$, the bounds for the j th neuron of layer i can be iteratively tightened in separate LP calls. However, this highly constrained program is too expensive to be run multiple times for each neuron in a neural network.

Inspired by the success of CROWN-family robustness verifiers Zhang et al. [2018], Xu et al. [2021], Wang et al. [2021], Zhang et al. [2022], we efficiently provide lower bounds to the program by optimizing its Lagrangian dual. This dual is highly structured, allowing us to formulate quantities such as the input cutting plane and intermediate bounds as closed-form expressions of the dual variables. Our main generalization of the existing method is the ability to optimize variables with

respect to constraints that are sequentially **after** it in the neural network. We present this contribution in the following theorem.

Theorem 1 (Bounding cutting plane). *Given an output set $\mathcal{S}_{out} = \{\mathbf{y} : \mathbf{H}\mathbf{y} + \mathbf{d} \leq \mathbf{0}\}$ and vector \mathbf{c} , $g_c(\alpha, \gamma)$ is a lower bound to the linear program in (3) for $\mathbf{0} \leq \alpha \leq \mathbf{1}$, $\gamma \geq \mathbf{0}$, and g_c defined via*

$$\begin{aligned} g_c(\alpha, \gamma) &= \text{ReLU} \left(\mathbf{c} - \boldsymbol{\nu}^{(1)\top} \mathbf{W}^{(1)} \right) \mathbf{l}^{(0)} \\ &\quad - \text{ReLU} \left(-\mathbf{c} + \boldsymbol{\nu}^{(1)\top} \mathbf{W}^{(1)} \right) \mathbf{u}^{(0)} \\ &\quad - \sum_{i=1}^L \boldsymbol{\nu}^{(i)\top} \mathbf{b}^{(i)} + \sum_{i=1}^{L-1} \sum_{j \in \mathcal{I}^{\pm(i)}} \left[\frac{u_j^{(i)} l_j^{(i)} [\hat{\nu}_j^{(i)}]_+}{u_i^{(j)} - l_i^{(j)}} \right] \end{aligned}$$

where every term can be directly recursively computed via

$$\begin{aligned} \mathcal{I}^{-(i)} &= \{j : u_j^{(i)} \leq 0\} \text{ (Provably Off ReLUs)} \\ \mathcal{I}^{+(i)} &= \{j : l_j^{(i)} \geq 0\} \text{ (Provably On ReLUs)} \\ \mathcal{I}^{\pm(i)} &= \{j : l_j^{(i)} < 0 < u_j^{(i)}\} \text{ (Ambiguous ReLUs)} \\ \boldsymbol{\nu}^{(L)} &= -\gamma \\ \boldsymbol{\nu}^{(i)} &= \left(\mathbf{W}^{(i+1)\top} \right) \boldsymbol{\nu}^{(i+1)} \quad \forall i \in [L-1] \\ \nu_j^{(i)} &= \begin{cases} \hat{\nu}_j^{(i)}, & j \in \mathcal{I}^{+(i)} \\ 0, & j \in \mathcal{I}^{-(i)} \\ \frac{u_j^{(i)}}{u_i^{(j)} - l_i^{(j)}} [\hat{\nu}_j^{(i)}]_+ - \alpha_j^{(i)} [\hat{\nu}_j^{(i)}]_-, & j \in \mathcal{I}^{\pm(i)} \end{cases} \quad \forall i \in [L-1] \end{aligned}$$

Proof. Full proof is presented in Appendix B. \square

In Appendix A, we show how to also compute bounds on the values of intermediate neurons in the network using a similar approach. Since the intermediate bounds might depend on bounds on neurons in subsequent layers (due to the output constraint), we cannot simply optimize bounds in a single forward pass layer by layer, unlike prior work [Zhang et al., 2022]. Instead, we must iteratively tighten these bounds, where in each pass all bounds are tightened given the tightest bounds on all neurons computed thus far. This iterative approach is able to tighten the bounds by several orders of magnitude, as shown in Figure 5. After performing this procedure once, the intermediate bounds can be used to tightly lower bound $\mathbf{c}^\top \mathbf{x}$ for any \mathbf{c} via Theorem 1. Therefore, this computation can be shared across all the constraints \mathbf{c} we use to describe \mathcal{S}_{over} . Our algorithm can be expressed in terms of forward/backward passes through layers of the neural network and implemented via standard deep learning modules in libraries like PyTorch [Paszke et al., 2019]. Since all of the operations are auto-differentiable, we can tighten our lower bound using standard gradient ascent (projected by the dual variable constraints).

Connection to forward verification Our bound in Theorem 1 introduces the dual variable γ , which enforces the output constraint during optimization. In fact, we can use this variable to get a better conceptual interpretation of our result. Consider the optimization problem in (1). Dualizing the output constraint and taking the dual wrt the constraint $\mathbf{H}f(\mathbf{x}) + \mathbf{d} \leq \mathbf{0}$ yields the following lower bound:

$$\begin{aligned} \max_{\gamma} \min_{\mathbf{x}} \quad & \mathbf{c}^\top \mathbf{x} + \gamma^\top (\mathbf{H}f(\mathbf{x}) + \mathbf{d}) \\ \text{s.t.} \quad & \mathbf{x} \in \mathcal{X}; \quad \gamma \geq 0 \end{aligned}$$

The objective for the inner minimization can be represented as minimizing a linear function of the output of a residual neural network with a skip connection from the input to the output layer, subject to constraints on the input. This is precisely the standard forward verification problem.¹ This unifies the inverse verification problem with the forward verification problem, connecting our method to standard tools Brix et al. [2023], Xu et al. [2021], Ferrari et al. [2022]. For example, as long as f is a

¹Similarly, optimizing an intermediate bound is equivalent to a skip connection from layer i to the output.

Algorithm 1 INVPROP. Can be applied to branches to generate non-convex overapproximations. Lower and upper bound of all neurons and all constraints are optimized using distinct α and γ values in g .

```

Initialize  $\mathbf{l}^{(i)}, \mathbf{u}^{(i)}$  via cheap bound propagation methods for the forward verification problem
while lower bounds  $\mathbf{l}_c$  for  $\mathbf{c}^\top \hat{\mathbf{x}}^{(0)}$  are improving do
  for  $i \in \{L-1, L-2, \dots, 1, 0\}$  do
    for  $j \in$  layer  $i$  neurons,  $b \in \{\text{lower, upper}\}$  do
      Set  $g = g_{ij}^b$  in theorem 1 to optimize bound on neuron  $j$  in layer  $i$  with sense  $b$  (lower/upper)
      Optimize  $g_{ij}^b(\alpha_{i,j}, \gamma_{i,j})$  with gradient ascent
      if  $b=\text{upper}$  then
        Update  $u_j^{(i)}$  with negated optimum of ascent
      else
        Update  $l_j^{(i)}$  with optimum of ascent
      end if
    end for
  end for
  Update  $\mathbf{l}_c$  based on updated bounds using gradient ascent on  $g_c$ 
end while

```

general computation graph with ReLU activations, Auto-LiRPA Xu et al. [2020] can be used to lower bound the objective function with a closed form expression parameterized by relaxation variables α . With this, we can directly optimize our lower bound with respect to α, γ .

When f is a feedforward ReLU network, the lower bound described in this section is precisely the same as Theorem 1 (since both are solving the dual of the same linear program). This shows that the introduction of γ constitutes our generalization to the bound propagation framework.

3.3 Branch and Bound

Our current formulation still faces two sources of looseness: the gap in $\mathcal{S}_{\text{LP}} \supseteq \mathcal{S}_{\text{MILP}}$ and the gap in $\mathcal{S}_{\text{MILP}} \supseteq f^{-1}(\mathcal{S}_{\text{out}})$. To overcome both of these issues, we can make use of branching. While there are several possibilities here, we focus on input branching, which gave the biggest empirical gains in our experiments described in Section 4. More concretely, we divide the input domain $\mathcal{X} = [\mathbf{l}^{(0)}, \mathbf{u}^{(0)}]$ into several regions by choosing a coordinate i and computing

$$\mathcal{X}_a = \mathcal{X} \cap \{\mathbf{x} : \mathbf{x}_i \geq s_i\}, \mathcal{X}_b = \mathcal{X} \cap \{\mathbf{x} : \mathbf{x}_i \leq s_i\}$$

so that $\mathcal{X} = \mathcal{X}_a \cup \mathcal{X}_b$. Doing this recursively, we obtain several regions and can compute an overapproximation of $f^{-1}(\mathcal{S}_{\text{out}})$ when the input is in each of those regions, and take a union of the resulting sets. The finer the input domain we compute the over-approximation over, the tighter the approximation is.

4 Results

We demonstrate the impact of our approach on a controls benchmark Rober et al. [2022a,b] and OOD detection. For the established controls benchmark, we significantly outperform the state-of-the-art.

We measure the tightness of an over-approximation using its Approximation Ratio, defined as $\frac{\text{vol}(\mathcal{S}_{\text{over}})}{\text{vol}(f^{-1}(\mathcal{S}_{\text{out}}))}$. Both of these volumes are heuristically estimated with 1 million evenly distributed samples of the input space.

While INVPROP allows the optimization of arbitrary cutting planes, all experiments were performed using 40 planes with slopes of equally distributed angles. All implementation details are described in Section D.

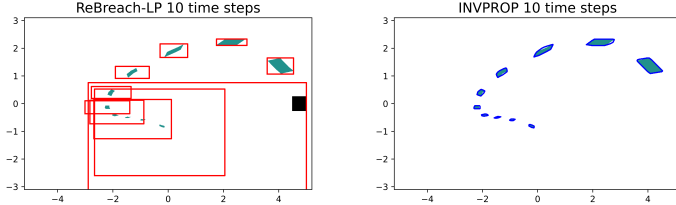


Figure 4: In both of the above plots, we over-approximate the set of states that would collide with the obstacle (black square) at $[4.5, 5.0] \times [-0.25, 0.25]$. We carry out this task for up to 10 steps back in time. Each green region is an approximation of the preimages sets via 1 million samples. The error of ReBreach-LP exponentially blows up further back in time while our bounding polytopes of 40 edges continue to stay at near perfect tightness.

Table 1: Comparison of our method vs SOTA in bounding the inputs that will collide with an obstacle in 10 time steps (as shown in Figure 4). We observe that we are significantly tighter and faster than their method.

METHOD	INPUT BRANCHING	APPROX RATIO	TIME (SEC)
REBREACH-LP	YES	4021.47	42.86 ± 0.04
INVPROP	NO	1.46	17.89 ± 0.03

4.1 Backward Reachability Analysis for Neural Feedback Loops

After combining (see Section D.2) the state-feedback control policy π of the benchmark with the state transition function (see Section 2.3), we get a three layer MLP with 12, 7, and 2 neurons which is typical for applications in this setting. We model multiple time steps via composing copies of this function. For example, the 10 time step transition function can be represented as a 21 layer MLP (after fusing consecutive linear layers in the composition). Moreover, we leverage the fact that intermediate bounds for the t time step transition can be used for the $t + 1$ time step transition.

We find that INVPROP is significantly tighter and faster than ReBreach-LP, the SOTA available method for this problem Rober et al. [2022a,b]. As evident in Figure 4, ReBreach-LP suffers from increasingly weak bounds as t increases, whereas our approach is able to compute tight bounds for all t . Different to their implementation, we are able to factor in the output constraint to improve the intermediate neuron bounds (see Figure 6). Furthermore, we can iteratively tighten these bounds with respect to each other. Even though we optimize many more quantities, our efficient bound propagation allows us to solve the problem faster overall. Figure 5 visualizes the improvement of the approximation ratio score and intermediate bounds over time. We also support the partitioning over the input space introduced by Rober et al. 2022a and the polytope bounds introduced by Everett et al. 2022. Both our increased tightness and speed are quantified in Table 1.

4.2 OOD Detection

Consider the calibrated OOD detector presented in Figure 1, encoded by a four layer MLP with 200, 200, 3, and 2 neurons. We compute the set of inputs which induce a sufficiently high ID confidence (measured by $\max\{y_0, y_1\} > y_2$), pictured in green in Figure 7. This set is non-convex, making the convex hull a poor over-approximation. With some simple input space branching, we can get a much tighter over-approximation, as shown in the right plot. We compare the performance of our approach with and without branching over the input space with the MILP baseline (see Table 2).

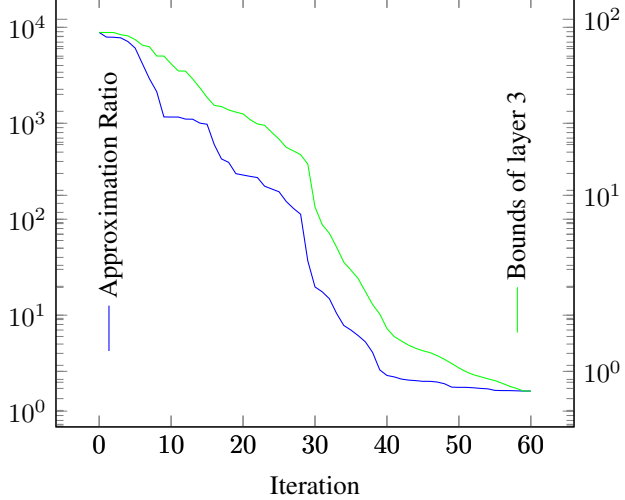


Figure 5: Our approach enables us to iteratively tighten the bounds of all layers, with each iteration allowing for a smaller approximation ratio with respect to the true preimage. Green: Sum of bound intervals for all neurons in the third layer (second hidden layer); Blue: resulting approximation ratio. Measured for step $t = 10$ of the control benchmark. One iteration updates all bounds of layers not previously optimized in step $t = 9$ as well as all cutting hyperplanes. Note that the improvement from iterative tightening is two orders of magnitude for intermediate bounds, and four orders of magnitude for the approximation ratio.

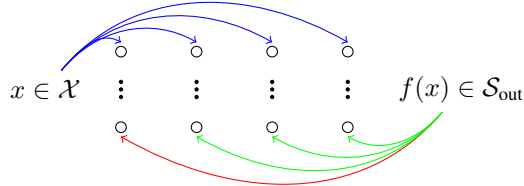


Figure 6: Comparison of constraints enforced in forward propagation, SOTA controls methods, and our approach. Forward propagation (blue arrows) cannot tighten intermediate bounds with respect to an output constraint. ReBreach-LP and DRIP (blue and red arrows) use the output constraint to tighten the input bounds, and use these input bounds to tighten the intermediate bounds. We (blue, red, and green arrows) tighten all intermediate bounds with respect to input and output constraints simultaneously.

5 Related Work

Formally Verified Neural Networks. There has been a large body of work on the formal verification of neural networks, tackling the problem from the angles of Interval Bound Propagation Gowal et al. [2018], Gehr et al. [2018], Convex Relaxations Wong and Kolter [2018], Shiqi et al. [2018], Salman et al. [2019], Dvijotham et al. [2018], Abstract Interpretation Singh et al. [2018], Linear Programming Ehlers [2017], Semidefinite Programming Raghunathan et al. [2018], Satisfiability Modulo Theories Katz et al. [2017], and Mixed Integer Linear Programming Tjeng et al. [2017]. However, most of this work is in the different setting of forward verification. Our work strictly generalizes the bound propagation framework presented in Xu et al. 2021 since setting $\gamma = 0$ in Theorem 1 recovers its results.

Formal Verification for Neural Feedback Loops. Our work was motivated by the growing body of work on backward reachability analysis and over-approximating states that result in a target set Everett et al. [2021]. The original method solely utilized input constraints for deriving intermediate bounds. The later development of Everett et al. 2022 improved upon this by optimizing $l^{(0)}$ and $u^{(0)}$

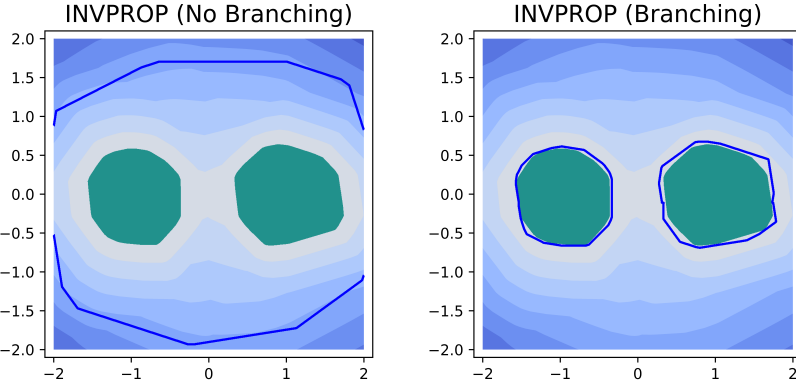


Figure 7: In both plots, the green regions approximate inputs which the model believes are in-distribution (generated from 1 million samples). On the left, the blue border traces out the intersection of the half-spaces we tightened without branching. On the right, we do the same with input space branching and display the union of multiple sets. We observe that branching produced a tighter and more expressive over-approximation.

Table 2: Comparison of methods for over-approximating the preimage of the OOD region shown in Figure 1 using 40 half-spaces.

METHOD	INPUT BRANCHING	APPROX RATIO	TIME (SEC)
MILP	NO	1.47	1562.26
INVPROP	NO	4.39	3.77 ± 0.02
INVPROP	YES	1.14	12.02 ± 0.06

with respect to output bounds. The work of Vincent and Schwager 2021 explores utilizing an LP with complete neuron branching to verify control safety, which can be viewed as a domain-specific implementation of our MILP formulation of the inverse verification problem. Both approaches share the ability to be terminated at any time for a looser approximation.

Certified OOD detection. There is a wide variety of OOD detection systems Yang et al. [2021], Salehi et al. [2022]. Commonly, they are evaluated empirically based on known OOD data Wang et al. [2022], Liang et al. [2018], Chen et al. [2021]. Therefore, they fail to provide verified guarantees for their effectiveness. In fact, many OOD detection systems are susceptible to adversarial attacks Sehwag et al. [2019], Chen et al. [2022]. Meinke et al. [2021] show how to verify robustness to adversarial examples around given input samples. Berrada et al. [2021] develop a general framework for certifying properties of output distributions of neural networks given constraints on the input distribution. They study the problem of distributionally robust OOD detection, where OOD data can be perturbed by noise drawn from a collection of distributions. However, this work is still constrained to verifying properties of the outputs given constraints (albeit probabilistic) on the inputs. In contrast, INVPROP is able to certify arbitrary regions of the input space that lead to confident predictions.

6 Discussion

In this work we present the challenge of over-approximating neural network preimages and provide an efficient algorithm to solve it. By doing so, we demonstrate strong performance on multiple application areas. This work provides a first attempt at this problem and we believe there is a large scope for future investigation and new applications of our contribution.

Limitations Our current implementation does not implement neuron and output branching. The input branching strategy we implemented will be less effective for high dimensional inputs.

Future Work To scale this verification to higher-dimensional tasks such as standard image datasets would require addressing additional challenges. The preimage may not be well represented by the intersection of half-spaces. Moreover, the difficulty of uniformly sampling cutting planes c will complicate measuring the efficacy of our methods.

Potential Negative Social Impact Our work improves reliable ML through facilitating the deployment of systems that provably align with practitioner expectations. As such, we expect INVPROP to have positive societal impact. We acknowledge that our improvements to verification may be repurposed as improvements to attacks given access to a model though we believe the positive use cases of our technique greatly outweigh current speculation of misusage.

7 Acknowledgements

We thank Michael Everett and Nicholas Rober for helpful discussion and feedback on the paper.

References

Leonard Berrada, Sumanth Dathathri, Krishnamurthy Dvijotham, Robert Stanforth, Rudy R Bunel, Jonathan Uesato, Sven Gowal, and M Pawan Kumar. Make sure you’re unsure: A framework for verifying probabilistic specifications. *Advances in Neural Information Processing Systems*, 34: 11136–11147, 2021.

Dimitri P. Bertsekas. *Dynamic Programming and Optimal Control*. Athena Scientific, 2nd edition, 2000. ISBN 1886529094.

Stephen Boyd, Stephen P Boyd, and Lieven Vandenberghe. *Convex optimization*. Cambridge University Press, 2004.

Christopher Brix, Mark Niklas Müller, Stanley Bak, Taylor T. Johnson, and Changliu Liu. First three years of the international verification of neural networks competition (vnn-comp), 2023. URL <https://arxiv.org/abs/2301.05815>.

Jiefeng Chen, Yixuan Li, Xi Wu, Yingyu Liang, and Somesh Jha. Atom: Robustifying out-of-distribution detection using outlier mining. In *Proceedings of European Conference on Machine Learning and Principles and Practice of Knowledge Discovery in Databases (ECML PKDD)*, 2021.

Jiefeng Chen, Yixuan Li, Xi Wu, Yingyu Liang, and Somesh Jha. Robust out-of-distribution detection for neural networks. In *The AAAI-22 Workshop on Adversarial Machine Learning and Beyond*, 2022. URL https://openreview.net/forum?id=WMIOz70_DPz.

Krishnamurthy Dvijotham, Robert Stanforth, Sven Gowal, Timothy A Mann, and Pushmeet Kohli. A dual approach to scalable verification of deep networks. In *UAI*, volume 1, page 3, 2018.

Ruediger Ehlers. Formal verification of piece-wise linear feed-forward neural networks. In *International Symposium on Automated Technology for Verification and Analysis*, pages 269–286. Springer, 2017.

Michael Everett, Golnaz Habibi, Chuangchuang Sun, and Jonathan P How. Reachability analysis of neural feedback loops. *IEEE Access*, 9:163938–163953, 2021.

Michael Everett, Rudy Bunel, and Shayegan Omidshafiei. Drip: Domain refinement iteration with polytopes for backward reachability analysis of neural feedback loops. *arXiv preprint arXiv:2212.04646*, 2022.

Claudio Ferrari, Mark Niklas Mueller, Nikola Jovanović, and Martin Vechev. Complete verification via multi-neuron relaxation guided branch-and-bound. In *International Conference on Learning Representations*, 2022. URL https://openreview.net/forum?id=l_amHf1oaK.

Timon Gehr, Matthew Mirman, Dana Drachsler-Cohen, Petar Tsankov, Swarat Chaudhuri, and Martin Vechev. Ai2: Safety and robustness certification of neural networks with abstract interpretation. In *2018 IEEE Symposium on Security and Privacy (SP)*, pages 3–18, 2018. doi: 10.1109/SP.2018.00058.

Sven Gowal, Krishnamurthy Dvijotham, Robert Stanforth, Rudy Bunel, Chongli Qin, Jonathan Uesato, Relja Arandjelovic, Timothy Mann, and Pushmeet Kohli. On the effectiveness of interval bound propagation for training verifiably robust models. *arXiv preprint arXiv:1810.12715*, 2018.

Dan Hendrycks, Mantas Mazeika, and Thomas Dietterich. Deep anomaly detection with outlier exposure. *arXiv preprint arXiv:1812.04606*, 2018.

Haimin Hu, Mahyar Fazlyab, Manfred Morari, and George J. Pappas. Reach-sdp: Reachability analysis of closed-loop systems with neural network controllers via semidefinite programming. In *2020 59th IEEE Conference on Decision and Control (CDC)*, pages 5929–5934, 2020. doi: 10.1109/CDC42340.2020.9304296.

Guy Katz, Clark Barrett, David L Dill, Kyle Julian, and Mykel J Kochenderfer. Reluplex: An efficient smt solver for verifying deep neural networks. In *International conference on computer aided verification*, pages 97–117. Springer, 2017.

Shiyu Liang, Yixuan Li, and R. Srikant. Enhancing the reliability of out-of-distribution image detection in neural networks. In *International Conference on Learning Representations*, 2018. URL <https://openreview.net/forum?id=H1VGkIxRZ>.

Alexander Meinke, Julian Bitterwolf, and Matthias Hein. Provably robust detection of out-of-distribution data (almost) for free. *arXiv preprint arXiv:2106.04260*, 2021.

Adam Paszke, Sam Gross, Francisco Massa, Adam Lerer, James Bradbury, Gregory Chanan, Trevor Killeen, Zeming Lin, Natalia Gimelshein, Luca Antiga, Alban Desmaison, Andreas Kopf, Edward Yang, Zachary DeVito, Martin Raison, Alykhan Tejani, Sasank Chilamkurthy, Benoit Steiner, Lu Fang, Junjie Bai, and Soumith Chintala. Pytorch: An imperative style, high-performance deep learning library. In *Advances in Neural Information Processing Systems 32*, pages 8024–8035. Curran Associates, Inc., 2019. URL <http://papers.neurips.cc/paper/9015-pytorch-an-imperative-style-high-performance-deep-learning-library.pdf>.

Aditi Raghunathan, Jacob Steinhardt, and Percy Liang. Certified defenses against adversarial examples. *arXiv preprint arXiv:1801.09344*, 2018.

Nicholas Rober, Michael Everett, Songan Zhang, and Jonathan P How. A hybrid partitioning strategy for backward reachability of neural feedback loops. *arXiv preprint arXiv:2210.07918*, 2022a.

Nicholas Rober, Sydney M Katz, Chelsea Sidrane, Esen Yel, Michael Everett, Mykel J Kochenderfer, and Jonathan P How. Backward reachability analysis of neural feedback loops: Techniques for linear and nonlinear systems. *arXiv preprint arXiv:2209.14076*, 2022b.

Mohammadreza Salehi, Hossein Mirzaei, Dan Hendrycks, Yixuan Li, Mohammad Hossein Rohban, and Mohammad Sabokrou. A unified survey on anomaly, novelty, open-set, and out of-distribution detection: Solutions and future challenges. *Transactions on Machine Learning Research*, 2022. URL <https://openreview.net/forum?id=aRtjVZvbpK>.

Hadi Salman, Greg Yang, Huan Zhang, Cho-Jui Hsieh, and Pengchuan Zhang. A convex relaxation barrier to tight robustness verification of neural networks. *Advances in Neural Information Processing Systems*, 32, 2019.

Vikash Sehwag, Arjun Nitin Bhagoji, Liwei Song, Chawin Sitawarin, Daniel Cullina, Mung Chiang, and Prateek Mittal. Analyzing the robustness of open-world machine learning. In *Proceedings of the 12th ACM Workshop on Artificial Intelligence and Security*, AISec’19, page 105–116, New York, NY, USA, 2019. Association for Computing Machinery. ISBN 9781450368339. doi: 10.1145/3338501.3357372. URL <https://doi.org/10.1145/3338501.3357372>.

Wang Shiqi, Kexin Pei, Whitehouse Justin, Junfeng Yang, and Suman Jana. Efficient formal safety analysis of neural networks. In *32nd Conference on Neural Information Processing Systems (NIPS)*, Montreal, Canada, 2018.

Gagandeep Singh, Timon Gehr, Matthew Mirman, Markus Püschel, and Martin Vechev. Fast and effective robustness certification. In S. Bengio, H. Wallach, H. Larochelle, K. Grauman, N. Cesa-Bianchi, and R. Garnett, editors, *Advances in Neural Information Processing Systems*, volume 31. Curran Associates, Inc., 2018. URL <https://proceedings.neurips.cc/paper/2018/file/f2f446980d8e971ef3da97af089481c3-Paper.pdf>.

Gagandeep Singh, Timon Gehr, Markus Püschel, and Martin Vechev. An abstract domain for certifying neural networks. *Proc. ACM Program. Lang.*, 3(POPL), jan 2019. doi: 10.1145/3290354. URL <https://doi.org/10.1145/3290354>.

Vincent Tjeng, Kai Xiao, and Russ Tedrake. Evaluating robustness of neural networks with mixed integer programming. *arXiv preprint arXiv:1711.07356*, 2017.

Joseph A. Vincent and Mac Schwager. Reachable polyhedral marching (rpm): A safety verification algorithm for robotic systems with deep neural network components. In *2021 IEEE International Conference on Robotics and Automation (ICRA)*, pages 9029–9035, 2021. doi: 10.1109/ICRA48506.2021.9561956.

Haoqi Wang, Zhizhong Li, Litong Feng, and Wayne Zhang. Vim: Out-of-distribution with virtual-logit matching. In *Proceedings of the IEEE/CVF Conference on Computer Vision and Pattern Recognition*, 2022.

Shiqi Wang, Huan Zhang, Kaidi Xu, Xue Lin, Suman Jana, Cho-Jui Hsieh, and J Zico Kolter. Beta-CROWN: Efficient bound propagation with per-neuron split constraints for complete and incomplete neural network verification. *Advances in Neural Information Processing Systems*, 34, 2021.

Eric Wong and Zico Kolter. Provable defenses against adversarial examples via the convex outer adversarial polytope. In *International Conference on Machine Learning*, pages 5286–5295. PMLR, 2018.

Kaidi Xu, Zhouxing Shi, Huan Zhang, Yihan Wang, Kai-Wei Chang, Minlie Huang, Bhavya Kailkhura, Xue Lin, and Cho-Jui Hsieh. Automatic perturbation analysis for scalable certified robustness and beyond. *Advances in Neural Information Processing Systems*, 33, 2020.

Kaidi Xu, Huan Zhang, Shiqi Wang, Yihan Wang, Suman Jana, Xue Lin, and Cho-Jui Hsieh. Fast and Complete: Enabling complete neural network verification with rapid and massively parallel incomplete verifiers. In *International Conference on Learning Representations*, 2021. URL <https://openreview.net/forum?id=nVZtXBI6LNn>.

Jingkang Yang, Kaiyang Zhou, Yixuan Li, and Ziwei Liu. Generalized out-of-distribution detection: A survey. *arXiv preprint arXiv:2110.11334*, 2021.

Huan Zhang, Tsui-Wei Weng, Pin-Yu Chen, Cho-Jui Hsieh, and Luca Daniel. Efficient neural network robustness certification with general activation functions. *Advances in Neural Information Processing Systems*, 31:4939–4948, 2018. URL <https://arxiv.org/pdf/1811.00866.pdf>.

Huan Zhang, Shiqi Wang, Kaidi Xu, Linyi Li, Bo Li, Suman Jana, Cho-Jui Hsieh, and J Zico Kolter. General cutting planes for bound-propagation-based neural network verification. *Advances in Neural Information Processing Systems*, 2022.

A Optimizing Intermediate Bounds

We first present a generalized theorem which provides a lower bound for any linear combination of $\hat{\mathbf{x}}^{(0)}$ and $\mathbf{x}^{(i)}$. We prove this theorem in Appendix B. We note that by selecting the coefficients of these variables (named $\mathbf{c}^{(i)}$ for $i \in \{0, 1, \dots, L-1\}$), we recover the two following functionalities which we name $g_c(\alpha, \gamma)$ and $g_{i,j}^b(\alpha, \gamma)$ (respectively).

- When the only nonzero coefficients are $\mathbf{c}^{(0)} = \mathbf{c}$, we recover Theorem 1. We refer to this bound as $g_c(\alpha, \gamma)$
- When the only nonzero coefficient is $c_j^{(i)} = 1$, we can lower bound $l_j^{(i)}$ by $g_{i,j}^{\text{lower}}(\alpha, \gamma)$. If we set $c_j^{(i)} = -1$, we can upper bound $u_j^{(i)}$ by $-g_{i,j}^{\text{upper}}(\alpha, \gamma)$.

With this, we present our generalized theorem.

Theorem 2 (Lower-bounding combination of neurons). *Given an output set $\mathcal{S}_{\text{out}} = \{\mathbf{y} : \mathbf{H}\mathbf{y} + \mathbf{d} \leq \mathbf{0}\}$ and vector \mathbf{c} , $g(\alpha, \gamma)$ is a lower bound to the linear program in (3) with objective $\mathbf{c}^{(0)\top} \hat{\mathbf{x}}^{(0)} + \sum_{i=1}^{L-1} \mathbf{c}^{(i)\top} \mathbf{x}^{(i)}$ for $\mathbf{0} \leq \alpha \leq \mathbf{1}$, $\gamma \geq \mathbf{0}$, and g defined via*

$$\begin{aligned} g(\alpha, \gamma) = & \text{ReLU} \left(\mathbf{c}^{(0)\top} - \boldsymbol{\nu}^{(1)\top} \mathbf{W}^{(1)} \right) \mathbf{l}^{(0)} \\ & - \text{ReLU} \left(-\mathbf{c}^{(0)\top} + \boldsymbol{\nu}^{(1)\top} \mathbf{W}^{(1)} \right) \mathbf{u}^{(0)} \\ & - \sum_{i=1}^L \boldsymbol{\nu}^{(i)\top} \mathbf{b}^{(i)} + \sum_{i=1}^{L-1} \sum_{j \in \mathcal{I}^{\pm(i)}} \left[\frac{u_j^{(i)} l_j^{(i)} [\hat{\nu}_j^{(i)}]_+}{u_i^{(j)} - l_i^{(j)}} \right] \end{aligned}$$

where every term can be directly recursively computed via

$$\begin{aligned} \mathcal{I}^{-(i)} &= \{j : u_j^{(i)} \leq 0\} \\ \mathcal{I}^{+(i)} &= \{j : l_j^{(i)} \geq 0\} \\ \mathcal{I}^{\pm(i)} &= \{j : l_j^{(i)} < 0 < u_j^{(i)}\} \\ \boldsymbol{\nu}^{(L)} &= -\gamma \\ \hat{\nu}_j^{(i)} &= \boldsymbol{\nu}^{(i+1)\top} \mathbf{W}_{:,j}^{(i+1)} \\ \nu_j^{(i)} &= \begin{cases} \hat{\nu}_j^{(i)} - c_j^{(i)}, & j \in \mathcal{I}^{+(i)} \\ -c_j^{(i)}, & j \in \mathcal{I}^{-(i)} \\ \frac{u_j^{(i)}}{u_i^{(j)} - l_i^{(j)}} [\hat{\nu}_j^{(i)}]_+ - \alpha_j^{(i)} [\hat{\nu}_j^{(i)}]_- + c_j^{(i)}, & j \in \mathcal{I}^{\pm(i)} \end{cases} \end{aligned}$$

B Dual Derivation

We now prove the generalized theorem.

As a conceptual overview of our proof, we take the Lagrange dual of the linear program to derive an unconstrained optimization problem. From here, we derive constraints that must be satisfied in the max min formulation. These constraints yield the bound propagation procedure we display in Theorem 1.

We start with the LP of the convex relaxation.

$$\begin{aligned}
\min_{\mathbf{x}, \hat{\mathbf{x}}, \mathbf{z}} \quad & \mathbf{c}^{(0)\top} \hat{\mathbf{x}}^{(0)} + \sum_{i=1}^{L-1} \mathbf{c}^{(i)\top} \mathbf{x}^{(i)} \\
\text{s.t.} \quad & \mathbf{l}^{(0)} \leq \hat{\mathbf{x}}^{(0)} \leq \mathbf{u}^{(0)} \\
& \mathbf{x}^{(L)} \leq \mathbf{0}; \\
& \mathbf{x}^{(i)} = \mathbf{W}^{(i)} \hat{\mathbf{x}}^{(i-1)} + \mathbf{b}^{(i)}; \quad i \in [L], \\
& \hat{x}_j^{(i)} \geq 0; j \in \mathcal{I}^{\pm(i)} \\
& \hat{x}_j^{(i)} \geq x_j^{(i)}; j \in \mathcal{I}^{\pm(i)} \\
& \hat{x}_j^{(i)} \leq u_j^{(i)} z_j^{(i)}; j \in \mathcal{I}^{\pm(i)} \\
& \hat{x}_j^{(i)} \leq x_j^{(i)} - l_j^{(i)} (1 - z_j^{(i)}); j \in \mathcal{I}^{\pm(i)} \\
& \hat{x}_j^{(i)} = x_j^{(i)}; j \in \mathcal{I}^{+(i)} \\
& \hat{x}_j^{(i)} = 0; j \in \mathcal{I}^{-(i)} \\
& 0 \leq z_j^{(i)} \leq 1; \quad j \in \mathcal{I}^{\pm(i)}, i \in [L]
\end{aligned}$$

From this, we take the Lagrange dual of most of the constraints. In doing so, we introduce a new dual variable for each constraint. Note that we do not dualize every constraint since they can easily be dealt with later.

$$\begin{aligned}
\min_{\mathbf{x}, \hat{\mathbf{x}}, \mathbf{z}} \quad & \max_{\boldsymbol{\nu}, \boldsymbol{\mu}, \boldsymbol{\tau}, \boldsymbol{\gamma}, \boldsymbol{\pi}, \boldsymbol{\lambda}} \quad \mathbf{c}^{(0)\top} \hat{\mathbf{x}}^{(0)} + \sum_{i=1}^{L-1} \mathbf{c}^{(i)\top} \mathbf{x}^{(i)} + \boldsymbol{\gamma}^\top \mathbf{x}^{(L)} + \sum_{i=1}^L \boldsymbol{\nu}^{(i)\top} (\mathbf{x}^{(i)} - \mathbf{W}^{(i)} \hat{\mathbf{x}}^{(i-1)} - \mathbf{b}^{(i)}) \\
& + \sum_{i=1}^{L-1} \sum_{j \in \mathcal{I}^{\pm(i)}} \left[\mu_j^{(i)} (-\hat{x}_j^{(i)}) + \tau_j^{(i)} (x_j^{(i)} - \hat{x}_j^{(i)}) \right. \\
& \left. + \lambda_j^{(i)} (\hat{x}_j^{(i)} - u_j^{(i)} z_j^{(i)}) + \pi_j^{(i)} (\hat{x}_j^{(i)} - x_j^{(i)} + l_j^{(i)} - l_j^{(i)} z_j^{(i)}) \right] \\
\text{s.t.} \quad & \mathbf{l}^{(0)} \leq \hat{\mathbf{x}}^{(0)} \leq \mathbf{u}^{(0)}; \quad \hat{x}_j^{(i)} = 0, j \in \mathcal{I}^{-(i)}; \quad \hat{x}_j^{(i)} = x_j^{(i)}, j \in \mathcal{I}^{+(i)}; \quad 0 \leq z_j^{(i)} \leq 1, j \in \mathcal{I}^{\pm(i)} \\
& \boldsymbol{\mu} \geq 0; \quad \boldsymbol{\tau} \geq 0; \quad \boldsymbol{\gamma} \geq 0; \quad \boldsymbol{\pi} \geq 0; \quad \boldsymbol{\lambda} \geq 0
\end{aligned}$$

Since we took the dual of a linear program, the solution to the min-max optimization is equivalent to the solution of the max-min optimization by strong duality. Therefore, we can solve the following program (equivalent up to rearrangement).

$$\begin{aligned}
& \max_{\boldsymbol{\nu}, \boldsymbol{\mu}, \boldsymbol{\tau}, \boldsymbol{\gamma}, \boldsymbol{\pi}, \boldsymbol{\lambda}} \min_{\mathbf{x}, \hat{\mathbf{x}}, \mathbf{z}} \quad \left(\boldsymbol{\nu}^{(L)} + \boldsymbol{\gamma} \right)^T \mathbf{x}^{(L)} + \left(\mathbf{c}^{(0)\top} - \boldsymbol{\nu}^{(1)\top} \mathbf{W}^{(1)} \right) \hat{\mathbf{x}}^{(0)} \\
& + \sum_{i=1}^{L-1} \sum_{j \in \mathcal{I}^{+(i)}} \left(\nu_j^{(i)} - \boldsymbol{\nu}^{(i+1)\top} \mathbf{W}_{:,j}^{(i+1)} + c_j^{(i)} \right) x_j^{(i)} + \sum_{i=1}^{L-1} \sum_{j \in \mathcal{I}^{-(i)}} \left(\nu_j^{(i)} + c_j^{(i)} \right) x_j^{(i)} \\
& + \sum_{i=1}^{L-1} \sum_{j \in \mathcal{I}^{\pm(i)}} \left[\left(\nu_j^{(i)} + \tau_j^{(i)} - \pi_j^{(i)} + c_j^{(i)} \right) x_j^{(i)} \right. \\
& + \left(-\boldsymbol{\nu}^{(i+1)\top} \mathbf{W}_{:,j}^{(i+1)} - \mu_j^{(i)} - \tau_j^{(i)} + \lambda_j^{(i)} + \pi_j^{(i)} \right) \hat{x}_j^{(i)} \\
& \left. + \left(-u_j^{(i)} \lambda_j^{(i)} - l_j^{(i)} \pi_j^{(i)} \right) z_j^{(i)} \right] \\
& - \sum_{i=1}^L \boldsymbol{\nu}^{(i)\top} \mathbf{b}^{(i)} + \sum_{i=1}^{L-1} \sum_{j \in \mathcal{I}^{\pm(i)}} \pi_j^{(i)} l_j^{(i)} \\
& \text{s.t. } \mathbf{l}^{(0)} \leq \hat{\mathbf{x}}^{(0)} \leq \mathbf{u}^{(0)}; \quad 0 \leq z_j^{(i)} \leq 1, j \in \mathcal{I}^{\pm(i)} \\
& \boldsymbol{\mu} \geq 0; \quad \boldsymbol{\tau} \geq 0; \quad \boldsymbol{\gamma} \geq 0; \quad \boldsymbol{\pi} \geq 0; \quad \boldsymbol{\lambda} \geq 0
\end{aligned}$$

We seek to remove the remaining constraints. We note that for $z_j^{(i)}$ constrained to $[0, 1]$, if the coefficient is positive, we should set $z_j^{(i)} = 0$. Otherwise, we should set $z_j^{(i)} = 1$ (if the coefficient is non-positive).

We also note that to minimize $(\mathbf{c}^{(0)\top} - \boldsymbol{\nu}^{(1)\top} \mathbf{W}^{(1)}) \hat{\mathbf{x}}^{(0)}$ subject to $\mathbf{l}^{(0)} \leq \hat{\mathbf{x}}^{(0)} \leq \mathbf{u}^{(0)}$, we can consider the choice we must make in each dimension. If the j th entry of the coefficient is positive, we should set $\hat{x}_j^{(0)} = l_j^{(0)}$. Otherwise, we should set $\hat{x}_j^{(0)} = u_j^{(0)}$.

We reflect these observations in the following program by replacing their terms by equivalent representations.

$$\begin{aligned}
& \max_{\boldsymbol{\nu}, \boldsymbol{\mu}, \boldsymbol{\tau}, \boldsymbol{\gamma}, \boldsymbol{\pi}, \boldsymbol{\lambda}} \min_{\mathbf{x}, \hat{\mathbf{x}}} \quad \left(\boldsymbol{\nu}^{(L)} + \boldsymbol{\gamma} \right)^T \mathbf{x}^{(L)} + \text{ReLU} \left(\mathbf{c}^{(0)\top} - \boldsymbol{\nu}^{(1)\top} \mathbf{W}^{(1)} \right) \mathbf{l}^{(0)} - \text{ReLU} \left(-\mathbf{c}^{(0)\top} + \boldsymbol{\nu}^{(1)\top} \mathbf{W}^{(1)} \right) \mathbf{u}^{(0)} \\
& + \sum_{i=1}^{L-1} \sum_{j \in \mathcal{I}^{+(i)}} \left(\nu_j^{(i)} - \boldsymbol{\nu}^{(i+1)\top} \mathbf{W}_{:,j}^{(i+1)} + c_j^{(i)} \right) x_j^{(i)} + \sum_{i=1}^{L-1} \sum_{j \in \mathcal{I}^{-(i)}} \left(\nu_j^{(i)} + c_j^{(i)} \right) x_j^{(i)} \\
& + \sum_{i=1}^{L-1} \sum_{j \in \mathcal{I}^{\pm(i)}} \left[\left(\nu_j^{(i)} + \tau_j^{(i)} - \pi_j^{(i)} + c_j^{(i)} \right) x_j^{(i)} \right. \\
& + \left(-\boldsymbol{\nu}^{(i+1)\top} \mathbf{W}_{:,j}^{(i+1)} - \mu_j^{(i)} - \tau_j^{(i)} + \lambda_j^{(i)} + \pi_j^{(i)} \right) \hat{x}_j^{(i)} \\
& \left. - \text{ReLU} \left(u_j^{(i)} \lambda_j^{(i)} + l_j^{(i)} \pi_j^{(i)} \right) \right] \\
& - \sum_{i=1}^L \boldsymbol{\nu}^{(i)\top} \mathbf{b}^{(i)} + \sum_{i=1}^{L-1} \sum_{j \in \mathcal{I}^{\pm(i)}} \pi_j^{(i)} l_j^{(i)} \\
& \text{s.t. } \boldsymbol{\mu} \geq 0; \quad \boldsymbol{\tau} \geq 0; \quad \boldsymbol{\gamma} \geq 0; \quad \boldsymbol{\pi} \geq 0; \quad \boldsymbol{\lambda} \geq 0
\end{aligned}$$

From here, we note that the variables \mathbf{x} or $\hat{\mathbf{x}}$ are unconstrained variables. Therefore, if any of their coefficients are nonzero, the inner minimization can immediately drive its value to $-\infty$. As such, the outer maximization must set all of these coefficients to zero. Therefore, we can derive constraints from this restructured optimization and remove the free variables $\mathbf{x}, \hat{\mathbf{x}}$.

$$\begin{aligned}
\max_{\boldsymbol{\nu}, \boldsymbol{\mu}, \boldsymbol{\tau}, \boldsymbol{\gamma}, \boldsymbol{\pi}, \boldsymbol{\lambda}} \quad & \text{ReLU} \left(\boldsymbol{c}^{(0)\top} - \boldsymbol{\nu}^{(1)\top} \mathbf{W}^{(1)} \right) \boldsymbol{l}^{(0)} - \text{ReLU} \left(-\boldsymbol{c}^{(0)\top} + \boldsymbol{\nu}^{(1)\top} \mathbf{W}^{(1)} \right) \boldsymbol{u}^{(0)} - \sum_{i=1}^L \boldsymbol{\nu}^{(i)\top} \mathbf{b}^{(i)} \\
& + \sum_{i=1}^{L-1} \sum_{j \in \mathcal{I}^{\pm(i)}} \left[\pi_j^{(i)} l_j^{(i)} - \text{ReLU} \left(u_j^{(i)} \lambda_j^{(i)} + l_j^{(i)} \pi_j^{(i)} \right) \right] \\
\text{s.t.} \quad & \boldsymbol{\nu}^{(L)} = -\boldsymbol{\gamma} \\
& \nu_j^{(i)} = \boldsymbol{\nu}^{(i+1)\top} \mathbf{W}_{:,j}^{(i+1)} - c_j^{(i)}, j \in \mathcal{I}^{+(i)} \\
& \nu_j^{(i)} = -c_j^{(i)}, j \in \mathcal{I}^{-(i)} \\
& \nu_j^{(i)} = \pi_j^{(i)} - \tau_j^{(i)} + c_j^{(i)}, j \in \mathcal{I}^{\pm(i)} \\
& \boldsymbol{\nu}^{(i+1)\top} \mathbf{W}_{:,j}^{(i+1)} = \left(\lambda_j^{(i)} + \pi_j^{(i)} \right) - \left(\mu_j^{(i)} + \tau_j^{(i)} \right), j \in \mathcal{I}^{\pm(i)} \\
& \boldsymbol{\mu} \geq 0; \quad \boldsymbol{\tau} \geq 0; \quad \boldsymbol{\gamma} \geq 0; \quad \boldsymbol{\pi} \geq 0; \quad \boldsymbol{\lambda} \geq 0
\end{aligned}$$

For the following, we define $\hat{\nu}_j^{(i)} = \boldsymbol{\nu}^{(i+1)\top} \mathbf{W}_{:,j}^{(i+1)}$. We note that since the upper and lower bounds of the neuron relaxation can not be tight simultaneously, at least one of $\lambda_j^{(i)} + \pi_j^{(i)}$ and $\mu_j^{(i)} + \tau_j^{(i)}$ must be non-zero². Therefore, we can write them as $\lambda_j^{(i)} + \pi_j^{(i)} = [\hat{\nu}_j^{(i)}]_+$ and $\mu_j^{(i)} + \tau_j^{(i)} = [\hat{\nu}_j^{(i)}]_-$

If we choose $\pi_j^{(i)} = \frac{u}{u-l} [\hat{\nu}_j^{(i)}]_+$ and $\lambda_j^{(i)} = \frac{-l}{u-l} [\hat{\nu}_j^{(i)}]_+$ and observe that $\tau_j^{(i)}$ lies in the interval 0 and $\hat{\nu}_j^{(i)}$, we get the following bound propagation procedure.

$$\begin{aligned}
\max_{\boldsymbol{\nu}, \boldsymbol{\alpha}, \boldsymbol{\gamma}} \quad & \text{ReLU} \left(\boldsymbol{c}^{(0)\top} - \boldsymbol{\nu}^{(1)\top} \mathbf{W}^{(1)} \right) \boldsymbol{l}^{(0)} - \text{ReLU} \left(-\boldsymbol{c}^{(0)\top} + \boldsymbol{\nu}^{(1)\top} \mathbf{W}^{(1)} \right) \boldsymbol{u}^{(0)} - \sum_{i=1}^L \boldsymbol{\nu}^{(i)\top} \mathbf{b}^{(i)} \\
& + \sum_{i=1}^{L-1} \sum_{j \in \mathcal{I}^{\pm(i)}} \left[\frac{u_j^{(i)} l_j^{(i)} [\hat{\nu}_j^{(i)}]_+}{u_i^{(j)} - l_i^{(j)}} \right] \\
\text{s.t.} \quad & \boldsymbol{\nu}^{(L)} = -\boldsymbol{\gamma} \\
& \nu_j^{(i)} = \boldsymbol{\nu}^{(i+1)\top} \mathbf{W}_{:,j}^{(i+1)} - c_j^{(i)}, j \in \mathcal{I}^{+(i)} \\
& \nu_j^{(i)} = -c_j^{(i)}, j \in \mathcal{I}^{-(i)} \\
& \hat{\nu}_j^{(i)} = \boldsymbol{\nu}^{(i+1)\top} \mathbf{W}_{:,j}^{(i+1)} \\
& \nu_j^{(i)} = \frac{u_j^{(i)}}{u_i^{(j)} - l_i^{(j)}} [\hat{\nu}_j^{(i)}]_+ - \alpha_j^{(i)} [\hat{\nu}_j^{(i)}]_- + c_j^{(i)}, j \in \mathcal{I}^{\pm(i)} \\
& \alpha_j^{(i)} \in [0, 1]; \quad \boldsymbol{\gamma} \geq 0
\end{aligned}$$

In this program, $\alpha_j^{(i)}$ are optimizable parameters controlling the relaxation of neuron j in layer i , similar to the ones appearing in Xu et al. 2021. γ , as discussed in the body of the paper, is the parameter which enforces the output constraint throughout this entire bound propagation procedure.

C Deriving Intermediate Bounds for Example 1

Preceding Constraints. The linear layer gives us $\boldsymbol{x}_0^{(1)} = \hat{\boldsymbol{x}}_0^{(0)}$. Since the only constraint we have is $\hat{\boldsymbol{x}}_0^{(0)} \in [-2, 2]$, the tightest intermediate bounds we can derive are $[-2, 2]$.

²Similar to the observation in Zhang et al. 2022, Wong and Kolter 2018, both may be non-zero in theory if our $l_j^{(i)}$ and $u_j^{(i)}$ are perfectly tight. However, this is rarely the case and loosening our bounds by an arbitrarily small constant suffices.

Following Constraints. Since the output of a ReLU is non-negative, we know that $\hat{x}_0^{(1)}, \hat{x}_1^{(1)} \geq 0$. Since $x_0^{(2)} = \hat{x}_0^{(1)} + \hat{x}_1^{(1)}$ and the output constraint enforces $x_0^{(2)} \leq 1.02$, we derive that $\hat{x}_0^{(1)} \leq 1.02$. If we set $\hat{x}_0^{(1)} = 1.02 - \hat{x}_1^{(1)}$, we see that $\hat{x}_0^{(1)}$ can take the entire interval $[0, 1.02]$. Since the only constraint we have on $x_0^{(1)}$ is that $\text{ReLU}(\hat{x}_0^{(1)}) = x^{(1)}$, our desired interval is the preimage of $[0, 1.02]$. This means that $x_0^{(1)}$ can take any value in the interval $(-\infty, 1.02]$.

All Constraints. We first note that by the first linear layer, we have $x_1^{(1)} = x_0^{(1)} + 1$. Therefore, if $x_0^{(1)}$ is less than 0, then $x_1^{(1)}$ is less than 1, which means $\text{ReLU}(x_0^{(1)}) + \text{ReLU}(x_1^{(1)})$ is less than 1, which contradicts the output constraint. If $x_0^{(1)}$ is always non-negative, then we have that the output is equivalent to $\text{ReLU}(x_0^{(1)}) + \text{ReLU}(x_0^{(1)} + 1) = 2x_0^{(1)} + 1$. Therefore, the output constraint implies $x_0^{(1)} \leq 0.01$. Any $x_0^{(1)} \in [0, 0.01]$ is achievable by setting the input to the desired value.

D Implementation

As stated in Algorithm 1, INVPROP first initializes bounds for all layers using some computationally cheap technique. Based on the input bounds given by \mathcal{X} , we first compute intermediate bounds using interval propagation and then tighten them based on the reverse symbolic interval propagation (RSIP) technique Singh et al. [2019]. While INVPROP will iteratively tighten those bounds over time, we found RSIP to reduce the total necessary runtime significantly compared to an initialization based solely on interval propagation. We initialize all α with 0.5 and all γ with 0.025.

The optimization is performed for all lower and upper bounds of all neurons in each layer in parallel, starting with the last layer and moving forward to the input layer. The bounds of the cutting hyperplanes are optimized last, together with the bounds on the input neurons. The improvements on $c^\top x$ are measured every 10th iteration. Before doing so, the bounds of the hyperplanes are tightened for 10 extra steps to improve their precision. We detect convergence by monitoring $c^\top x$. If successive iterations see minimal improvement, we stop or branch on the input space. All cutting hyperplanes are evenly distributed to maximize their information gain. For 40 hyperplanes in a 2D input space, we rotate each plane by 9° . All reported runtimes under 10 minutes are computed as the average of five runs.

D.1 Encoding Non-Linear Constraints

To support non-linear output sets, such as the maximum operation used in the OOD example in Section 4.2, the non-linearity needs to be encoded, such that it can be expressed as linear constraints over the modified network. We rewrite $\max(y_1, y_2) = \max(y_1 - y_2, 0) + y_2$ and add an additional ReLU layer for this operation. Note that to pass y_2 through this layer without modifying it, one can either write $y_2 = \max(y_2, 0) - \max(-y_2, 0)$, or $y_2 = \max(y_2 - M, 0) + M$ where M is the lower bound of all possible y_2 . We find that avoiding the additional ReLU relaxations that would occur for the first approach is beneficial for the optimization and compute a lower bound of M using interval propagation. As y_3 (for the OOD class) should not be changed by this operation either, we apply the same trick of subtracting and adding its lower bound.

D.2 Control Benchmark Encoding

We encode the entire control formula $x = \mathbf{A}x + \mathbf{B}u$ as one feedforward network by encoding the residual connection as regular fully connected layers. To this end, we use the same technique described in Section D.1 to shift the bounds into the positive regime, feed them forward and then shift them back.

To compute $\mathcal{S}_{\text{over}}$ for a timestep $t > 1$, we first stack the network t times, then simplify it by merging consecutive linear layers. All bounds of layers not affected by this merging that also appear in the network for $t - 1$ timesteps are reused. Their bounds are already tight enough and are not optimized further. Note that this is different than using the previous $\mathcal{S}_{\text{over}}$ as the new target region and using an unstacked network: All bounds of the new layers are still optimized w.r.t. the precise target \mathcal{S}_{out} . Therefore, we do not suffer from accumulating inaccuracies.

E Hardware

All CPU experiments were performed on a Dual Xeon Gold 6138. All GPU experiments were performed on a single NVIDIA V100 GPU.